

Computational drug repurposing for tuberculosis by inhibiting Ag85 complex proteins

Israini W. Iskandar¹, Astutiati Nurhasanah², Mohammad Hatta³, Firdaus Hamid³, Irda Handayani⁴, Ummi Chaera¹, Andi A. Yusriyah⁵, Balqis D. Jamaluddin¹, St Zaenab⁶, Najdah Hidayah⁷, Nihayatul Karimah², Andi D. Permana⁸ and Muhammad N. Massi^{3*}

¹Master Program of Biomedical Science, Postgraduate School, Universitas Hasanuddin, Makassar, Indonesia; ²Research and Innovation Agency (BRIN), Banten, Indonesia; ³Department of Clinical Microbiology, Faculty of Medicine, Universitas Hasanuddin, Makassar, Indonesia; ⁴Department of Clinical Pathology, Faculty of Medicine, Universitas Hasanuddin, Makassar, Indonesia; ⁵Department of Marine Science, Faculty of Marine Science and Fisheries, Universitas Hasanuddin, Makassar, Indonesia; ⁶Universitas Cokroaminoto Makassar, Makassar, Indonesia; ⁷Graduate School of Biomedical Sciences, Universitas Hasanuddin, Makassar, Indonesia; ⁸Faculty of Pharmacy, Universitas Hasanuddin, Makassar, Indonesia

*Corresponding author: nasrumm@unhas.ac.id

Abstract

Tuberculosis (TB) remains a significant and deadly infection among pulmonary diseases caused by *Mycobacterium tuberculosis*, a highly adaptive bacterium. The ability of *M. tuberculosis* to evade certain drugs has been linked to its unique structure, particularly in the cell envelope, where the Ag85 complex proteins play an essential role in this part. The aim of this study was to utilize a drug repurposing strategy targeting the Ag85 complex proteins. This study utilized a computational approach with 120 selected drugs experimentally identified to inhibit Tuberculosis. A virtual screening molecular docking with Autodock Vina was used to filter the compounds and identify the strong binders to the Ag85 Complex. Molecular dynamics simulations employed the Gromacs Packages to evaluate the stability of each complex, including root mean square deviation (RMSD), root mean square fluctuation (RMSF), and radius of gyration (RoG). Additionally, absorption, distribution, metabolism, excretion, and toxicity (ADMET) assessments were conducted to gather more information about the drug-likeness of each hit compound. Three compounds, selamectin, imatinib, and eltrombopag were selected as potential drugs repurposed to inhibit the activity of the Ag85 complex enzyme, with binding affinities ranging between -10.560 kcal/mol and -11.422 kcal/mol. The MD simulation within 100 ns (3 replicas) showed that the average RMSD of each Ag85A complex was 0.15 nm–0.16 nm, RMSF was 0.09 nm–0.10 nm, and RoG was 1.80 nm–1.81 nm. For Ag85B, the average RMSD was 1.79 nm–1.80 nm, RMSF was 0.08 nm–0.09 nm, and RoG was 1.79 nm – 1.80 nm. Then, for Ag85C, the mean RMSD was 0.16 nm–0.18 nm, RMSF was 0.09, and RoG was 1.77 nm. The study highlights that these promising results demonstrate the potential of some repurposed drugs in combating the Ag85 complex.

Keywords: Ag85 complex proteins, drug-repurposed, molecular docking, molecular dynamics, tuberculosis

Introduction

Tuberculosis (TB) is one of the leading pulmonary diseases, along with coronavirus disease 2019, and has been predicted to infect 10.8 million people in 2023 [1]. Although the occurrence of TB involves various factors, there are still many gaps that require further research, especially for its main agent, *Mycobacterium tuberculosis* [2]. *M. tuberculosis* is a type of bacillus bacteria



with a highly adaptive life cycle, enabling it to evade the host immune system, promoting its intracellular survival and residing in granulomas during its latent phase [3,4]. Several drugs have been used against *M. tuberculosis*, such as Rifampicin, Isoniazid, Delamanid, or Ethambutol, targeting the bacterial cell wall attachment of mycolic acid [5]. However, several reports indicate that cases of multiple-drug resistance (MDR) and extensive-drug resistance (XDR) are increasing in TB epidemics, involving several drugs commonly used for TB patients [6,7]. Previous studies have suggested that genes involved in the building resistance of *M. tuberculosis* against multiple drugs, such as Rifampicin and Isoniazid, include *katG*, *inhA*, *ahpC*, and *rpoB* [8,9].

The drug resistance of *M. tuberculosis* (a gram-positive bacillus) is linked to its thick, highly hydrophobic cell envelope. This is caused by the composition of the lipid layer and polysaccharide-mycolate complex, characterized by mycolic acid present on the surface of the cell wall [8,9]. This well-constructed cell wall feature is supported by the ability of *M. tuberculosis* to produce several specific proteins that facilitate bacterial survival, attachment, and manipulation of host targets during infection [10]. Some studies have reported that the major proteins secreted and potent antigens come from the antigen 85 complex (Ag85 Complex) [11]. The complex consists of three main proteins, namely Ag85A (Rv3804c/FbpA), Ag85B (Rv1886c/FbpB), and Ag85C (Rv0129c/FbpC) [11,12]. These proteins are enzymes that play an important role in cell-wall construction, acting as mycolyl transferases involved in the formation of trehalose monomycolate (TMM) and trehalose dimycolate (TDM) [13-15]. These enzymatic functions are vital for creating and altering key elements of the mycobacterial cell wall, which are crucial for *Mycobacterium tuberculosis*'s survival, disease progression, and eliciting host immune response [16,17]. All of these proteins can bind to a C-terminal pattern of the human fibronectin protein, suggesting their role in mediating bacterial attachment to host cells during infection [12].

Drug repurposing strategies could be employed to identify compounds with the likelihood of targeting the Ag85 complex and thus can be effective in attenuating the resistance of *M. tuberculosis* infection [18-20]. Even though there are numerous studies showed that repurposing existing drugs from 2010–2022 for TB, the mechanisms of these drugs remain unclear, particularly in relation to their interaction with Ag85 complex [21,22]. Herein, computational screenings were employed on previously reported compounds that were found to be active against *M. tuberculosis*. The aim of this study was to identify repurposed drugs with potential activities in targeting Ag85 complex, thus can be included in combinatorial therapies in TB management. Molecular docking and molecular dynamics (MD) simulation are strategic tools for drug repurposing investigations prior to in vitro or in vivo testing. The in silico methods offer several advantages, such as cost-effectiveness, reduced timeframes for screening potential candidates, and the ability to predict binding interactions and stability of compounds with the Ag85 complex.

Methods

System preparations

The crystal structures of the Ag85 complexes were obtained from the Protein Data Bank (PDB, <https://www.rcsb.org/>), comprising Ag85A (PDB ID: 1SFR) consisting of 288 amino acids (aa), Ag85B (PDB ID: 1FOP) composed of 284 aa, and Ag85C (PDB ID: 5OCJ) consisting of 275 aa. The resolutions of each protein were 2.7Å, 1.8Å, and 1.8Å, respectively. All three protein structures were prepared using UCSF Chimera version 1.17.3, PyMOL version 2.5.7, and ADFRsuite version 1.0 by removing all other heteroatoms, inhibitors, and water, adding hydrogen and minimizing the structure to enhance the accuracy of binding conformations. Considering the similar structures of Ag85 complexes, this study employed sequence alignment using Jalview version 2.11.3.2 to identify differences in the structures of each protein. It showed several differences in their amino acid sequences affecting their secondary structures (**Figure 1**). Ag85A has 18 loops, 9 alpha-helices, and 10 beta-strands (**Figure 2A**); Ag85B has 19 loops, 9 alpha-helices, and 10 beta-strands (**Figure 2B**); and Ag85C has 16 loops, 9 alpha-helices, and 8 beta-strands (**Figure 2C**). All three Ag85 complexes were superimposed, where the structures are presented in **Figure 2D**.

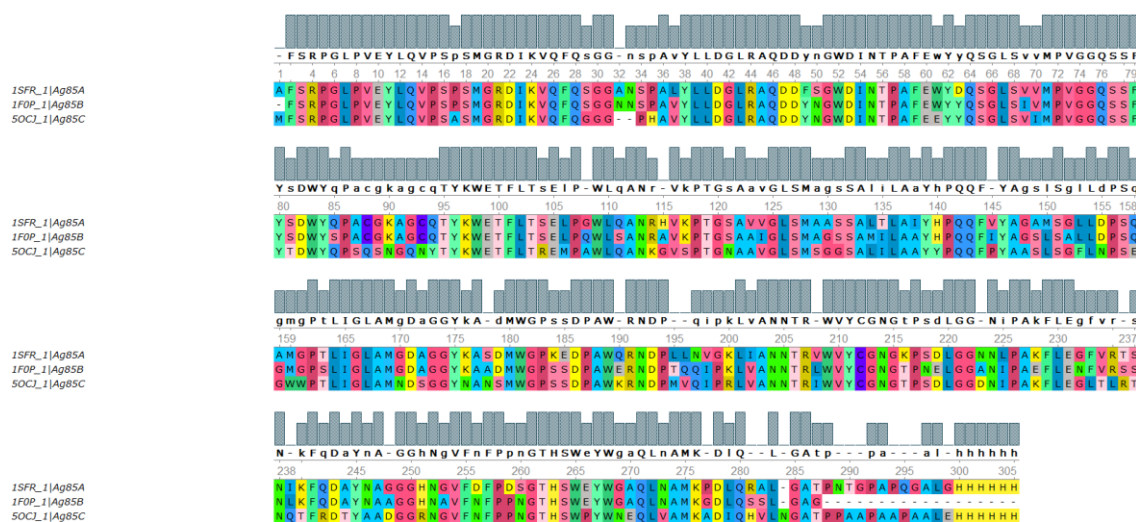


Figure 1. Sequence alignment of Ag85 complex protein.

The compound library of repurposed TB drugs, consisting of 120 compounds, was downloaded from the PubChem Database (<https://pubchem.ncbi.nlm.nih.gov/>) (see **Underlying data**) or drawn manually using Marvin Sketch software if the structure was not available in the database. The initial step in ligand preparation involved optimizing the geometry and adding hydrogen to each ligand using Marvin Sketch version 23.14. Particularly for the native ligands bound to the co-crystallized structures, such as Trehalose (Ag85B) and CyC (Ag85C), preparations were also carried out by extracting them from the PDB structures. Subsequently, all the ligands were prepared using ADFR Suite and Open Babel version 3.1.1 to convert the initial structure into pdbqt format for the molecular docking step.

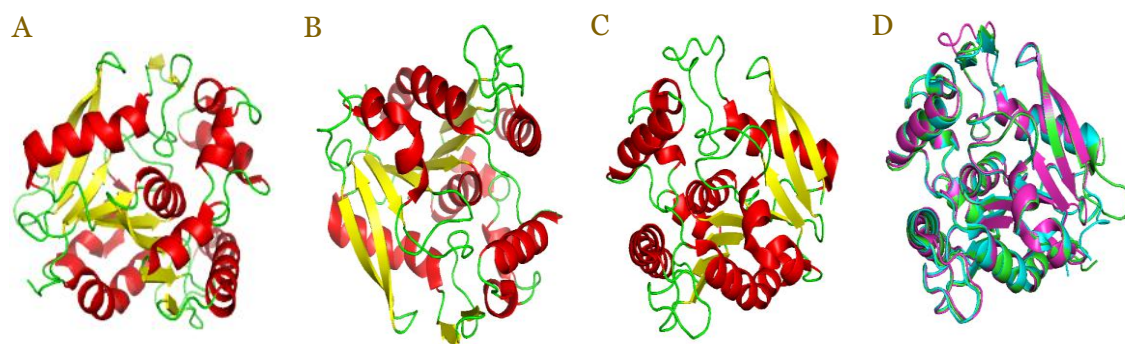


Figure 2. X-ray structures of Ag85A (PDB: 1SFR) (A), Ag85B (PDB: 1FoP) (B), and Ag85C (PDB: 5OCJ) (C), along with their superimposed structure (D). Loop, alpha-helix, and beta-sheet structures were presented in green, red, and yellow, respectively. In the superimposed structure for all the Ag85 complexes, green, blue, and magenta colors correspond to Ag85A, Ag85B, and Ag85C, respectively.

Molecular docking

The AutoDock Vina version 1.2.3 was employed for the molecular docking study [23,24]. The binding sites were determined based on the location of the native ligands for Ag85B and Ag85C. For Ag85B, the residues included Asp40, Gly41, Leu42, Arg43, Ala44, Leu125, Ser126, Met127, Asp170, Asn223, Pro225, Ala226, Leu229, His262, Ser263, Trp264 and Trp267, while the residues included at the binding site of Ag85C are Gly39, Leu40, Arg41, Leu123, Ser124, Met125, Pro223, Ala224, Leu227, His260, Trp262 and Trp265. Meanwhile, computed atlas of surface topography of proteins (CASTp) 3.0 (<http://sts.bioe.uic.edu/castp>) was employed to identify the binding pockets for the Ag85A protein, which involve the serine residues (124–126) due to the unavailability of the co-crystallized ligand in the structure [5]. To validate the docking position, re-docking of co-crystallized native ligands from Ag85B (PDB: 1FoP) and Ag85C (PDB: 5OCJ) was

performed. The re-docking was not performed for Ag85A (PDB: 1SFR) due to the absence of a native ligand. The grid center and the grid size of each complex used in the docking are presented in **Table 1**. The virtual screening was carried out by selecting the most potential ligands among the 120 compounds for drug repurposing against Ag85 complex proteins, explicitly considering their pose, binding energy, conformation, and any interactions between the receptor (protein) and its ligand (compound). Compounds with binding energies within ± 5 kcal/mol of the native ligands were classified as active. All the results of their conformations, poses, and structures were then analyzed using Discovery Studio Visualizer v21.1.0.20298, UCSF Chimera v1.17.3, and PyMOL v3.0.1 software.

Table 1. Grid parameters for each complex

Protein (receptor)	Grid center (x;y;z)	Grid box (x;y;z)
Ag85A (1SFR PDB)	50;58;6	20;20;20
Ag85B (1FoP PDB)	47;2;18	25;20;20
Ag85C (5OCJ PDB)	1;-23;-20	20;30;15

All units are reported in Å (Amstrong)

ADMET analysis

To obtain more information about the drug-like properties of the compounds, specifically regarding their absorption, distribution, metabolism, excretion, and toxicity (ADMET) properties, we performed an analysis using SwissADME (<http://www.swissadme.ch/>). The values were evaluated based on Lipinski's rule of five for drug-likeness. According to this rule, the logP should be ≤ 5 , the molecular weight (MW) should be ≤ 500 g/mol, and there should be a maximum of 10 hydrogen bond acceptors and a maximum of 5 hydrogen bond donors. Additionally, for rotatable bonds, the value should be under 10, with a polar surface area not exceeding 140 \AA^2 . For toxicity evaluation, the analyses were conducted using ADMETLab 2.0 (<https://admetmesh.scbdd.com/>).

Molecular dynamics

The best docking poses of the two most potential compounds from the docking study of each Ag85 complex were selected for the MD simulation. The entire system for MD simulation was performed using the CHARMM36 Force Field and SPC216 to build the solvent environment. Particularly for ligand topology, this study used SwissParam (<http://www.swissparam.ch/>), which utilizes the Merck Molecular Force Field (MMFF) based on the closest atom type in CHARMM36. Next, ions were added to the systems to achieve neutralization and were then minimized before being equilibrated in NPT and NVT conditions for 100 ps each. Then, the MD simulation was set up for 100 ns with three replicates for each complex and apo forms for Ag85 complex proteins. The results, such as root mean square deviation (RMSD), root mean square fluctuation (RMSF), and radius of gyration (RoG) were analyzed, and the visualizations were performed using PyMOL. In addition, the predicted binding free energy was estimated based on Molecular Mechanics–Poisson–Boltzmann Surface Area (MM-PBSA) method. The values of these parameters were then compared with those of native ligands.

Results

Docking results

The re-docking validation of the co-crystallized ligand was performed for Ag85B-Trehalose and Ag85C-methoxy-[(3- $\{R\}$)-3-[(2- $\{R\}$)-1-methoxy-1,3-bis(oxidanylidene)butan-2-yl]pentadecyl] phosphinic acid (CyC). Illustrations of the complex structures from the re-docking with the native ligands of Ag85B and Ag85C are presented in **Figure 3**. The binding affinities were -5.82 kcal/mol with four hydrogen bond interactions without van der Waals and hydrophobic interactions (RMSD: 1.12 \AA) and -6.84 kcal/mol (RMSD: 1.48 \AA), forming three hydrogen bonds, and three hydrophobic interactions (one pi-sigma, one alkyl and one pi-alkyl) for Ag85B and Ag85C, respectively.

The re-docking was not performed for Ag85A since it has no co-crystallized ligand. The molecular docking results showed competitive scores due to the compounds' high structural and

conformational similarity, which led to comparable binding poses within the cleft. The study results from the repurposed drug list (n=120 compounds) revealed that some compounds were identified to have binding affinities of more than -10 kcal/mol (**Underlying data**). For Ag85A, the scores ranged from 28.9 to -11.42 kcal/mol. Compounds with binding affinities of more than -10 kcal/mol are as follows: pranlukast (-10.93 kcal/mol), fluspirilene (-10.16 kcal/mol), pimoziide (-10.31 kcal/mol), eltrombopag (-10.44 kcal/mol), moxidectin (-10.55 kcal/mol), imatinib (-10.70 kcal/mol), and selamectin (-11.42 kcal/mol). Compounds with positive binding affinities in the interaction with Ag85A are rifabutin (1.11 kcal/mol), cyclosporine-A (14.13 kcal/mol), and vancomycin (28.94 kcal/mol).

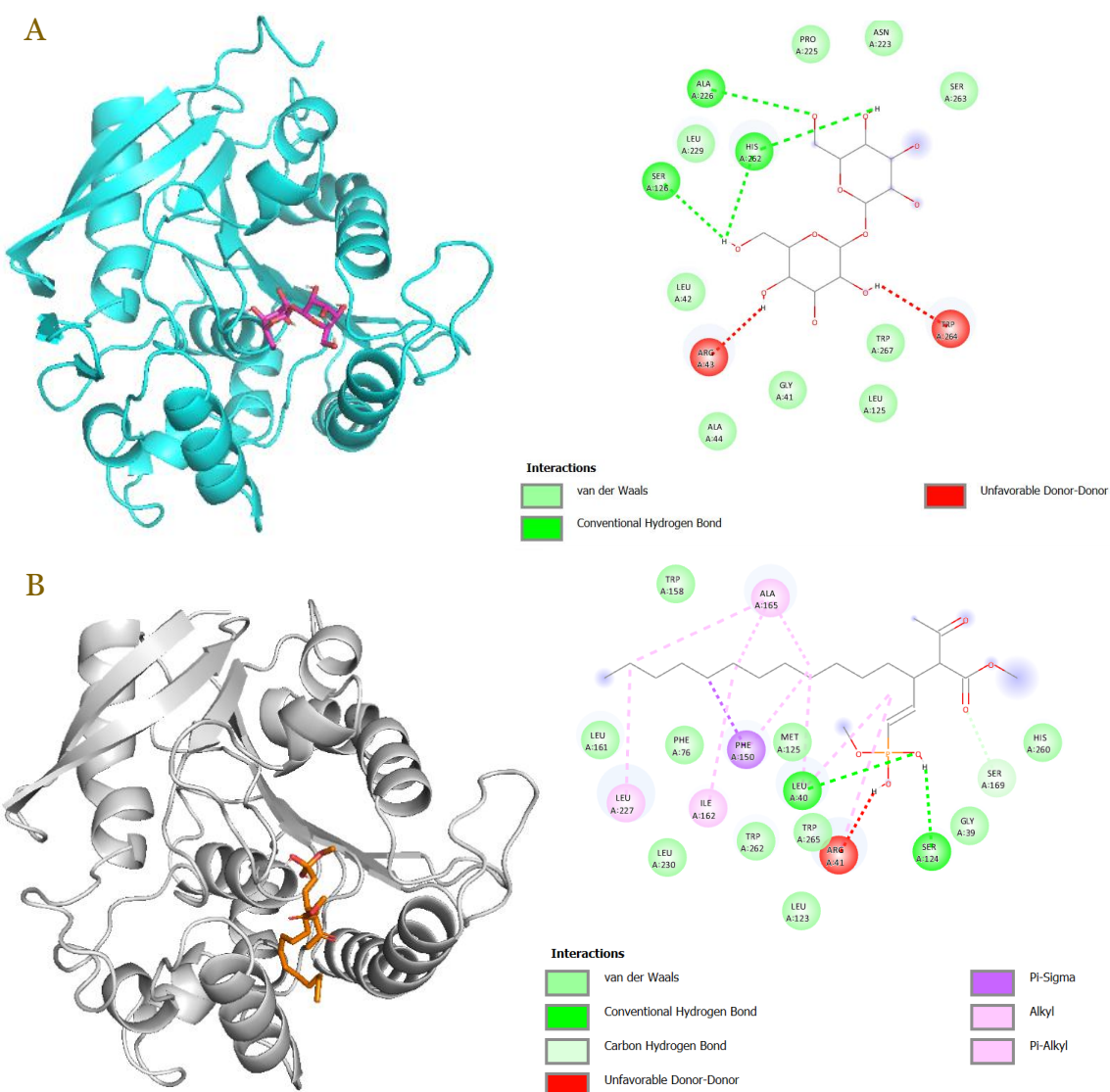


Figure 3. 3D visualization of protein-ligand structures from the re-docking of Ag85B (A) and Ag85C (B) with their native ligands (trehalose and CyC, respectively).

On the other hand, the docking results on Ag85B revealed that pimoziide (-10.98 kcal/mol), imatinib (-10.82 kcal/mol), eltrombopag (-10.93 kcal/mol), and imatinib (-10.98 kcal/mol) had the best docking scores. In contrast, cyclosporine-A and vancomycin had the worst scores of 5.37 kcal/mol and 9.36 kcal/mol for their interaction with Ag85B, respectively. Compared to Ag85A and Ag85B, ligands interacting with Ag85C have no positive binding affinities, where the values ranged from -2.93 to -11.14 kcal/mol. Interactions with pranlukast (-10.5 kcal/mol), imatinib (-10.55 kcal/mol), imatinib (-10.56 kcal/mol), and eltrombopag (-11.14 kcal/mol) were the most potential. Comparing the re-docking results from native ligands and the docking study of the listed repurposed drugs show significant differences in their scores. This suggests that the

repurposed drugs could interact strongly with their receptors, exhibiting higher binding affinity than the native ligands. From these results, we chose to focus on selamectin, imatinib, and eltrombopag due to their strong binding affinity (ranging from -10.560 to -11.422 kcal/mol) against at least one of the Ag85 proteins of *M. tuberculosis*.

An illustration of the Ag85A–selamectin complex from the docking simulation is presented in **Figure 4**. The docking score was -11.422 kcal/mol with interactions involving multiple residues such as Arg43, Ser126, Ala167, Pro225, Val233, Leu229, His262, and Trp264. Hydrogen bond interactions were observed particularly with Ser126 and Arg43, while other interactions, including alkyl and pi-alkyl, were formed with Pro225, Leu 229, Val233, His262, and Trp264. Additionally, this complex had an unfavorable bump with Ala167.

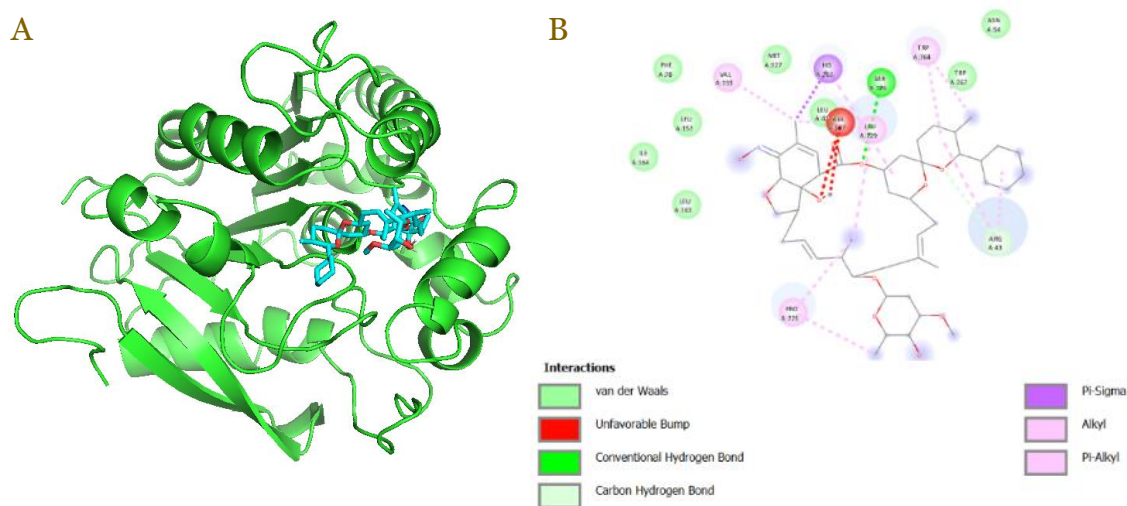


Figure 4. 3D visualization of selamectin forming complex with Ag85A (A). 2D representation of the Ag85A–selamectin complex with highlighted types of interaction and involved residues (B).

Imatinib demonstrates one of the highest binding affinities when interacting with Ag85B (-10.98 kcal/mol), Ag85A (-10.70 kcal/mol), and Ag85C (-10.56 kcal/mol) (**Figure 5**). Imatinib interaction with Ag85B involved residues such as Asp40, Gly41, Arg43, Leu42, Leu152, Leu163, Ile164, Leu166, Ala167, His262, and Leu229. Three hydrogen bonds establish the Ag85B–imatinib complex through Gly41 and Arg43 residues. When interacting with Ag85, imatinib forms several interactions with Asp40, Leu42, Arg43, Gln45, Leu152, Leu163, Ile164, Leu166, Ala167, Leu229, and Trp264. In the Ag85–imatinib complex, two hydrogen bonds were formed through Arg43 and Gln45 residues. Interactions of imatinib with Ag85C involved Leu40, Arg41, Phe150, Leu161, Ile162, Leu164, Ala165, and Leu227, where there is only one hydrogen bond was established through Arg41 (**Figure 5**).

The illustration for the Ag85C–eltrombopag complex generated by the docking simulation is presented in **Figure 6**. This complex was established with two hydrogen bonds involving Gly39 and Trp262 residues. Other residues of Ag85C, such as Ala165, Leu40, Leu227, Ile52, Arg41, and Phe150, also contributed to the complex formation via eight hydrophobic interactions. The simulated interaction of eltrombopag with Ag85B protein yielded four hydrogen bonds involving Ser126, His262, Trp264, and Leu42. Non-bonded interactions were also found in the Ag85B–eltrombopag complex via Arg43, Ile53, Leu229, and Ala167 residues.

Protein-ligand complex stability

The RMSDs for Ag85A–selamectin and Ag85A–imatinib stabilized at 60 ns, with values of 0.16 nm and 0.15 nm, respectively (**Figure 7**). The RMSDs for complexes involving Ag85B or Ag85C mostly stabilized at 10 ns. In comparison, the RMSDs of Ag85B and Ag85C complexes with their respective native ligands ranged from 0.14 to 0.17 nm (**Figure 7**). As for the RMSF, the average values across all complexes ranged from 0.07 to 0.1 nm (**Figure 8**). Complex with Ag85A as the protein, three prominent fluctuation peaks were identified at residues 88–91, 216–220, and 286–288 (**Figure 8**).

The interaction energies between all the Ag85 proteins and their respective ligands, encompassing Δ VDWAALS, Δ EEL, Δ ENPOLAR, Δ EPB, Δ EDISPER, Δ GGAS, and Δ GSOLV are presented in **Table 3**. The complex of Ag85A-selamectin demonstrates stronger binding affinity compared to Ag85A-gleevec, exhibiting more negative binding energies of -32.35 ± 3.30 kcal/mol and -9.27 ± 8.14 kcal/mol, respectively. Among Ag85B-complexes, Ag85B-eltrombopag exhibits a higher value of -21.55 ± 2.55 kcal/mol compared to Ag85B-gleevec and Ag85B-trehalose. Additionally, higher competing energies are observed within the Ag85C-complexes, particularly with Ag85C-eltromobopag (-21.52 ± 2.86 kcal/mol) and Ag85C-CyC (-22.21 ± 2.81 kcal/mol). As for Ag85B-imatinib, the total energy is -8.54 ± 3.86 kcal/mol.

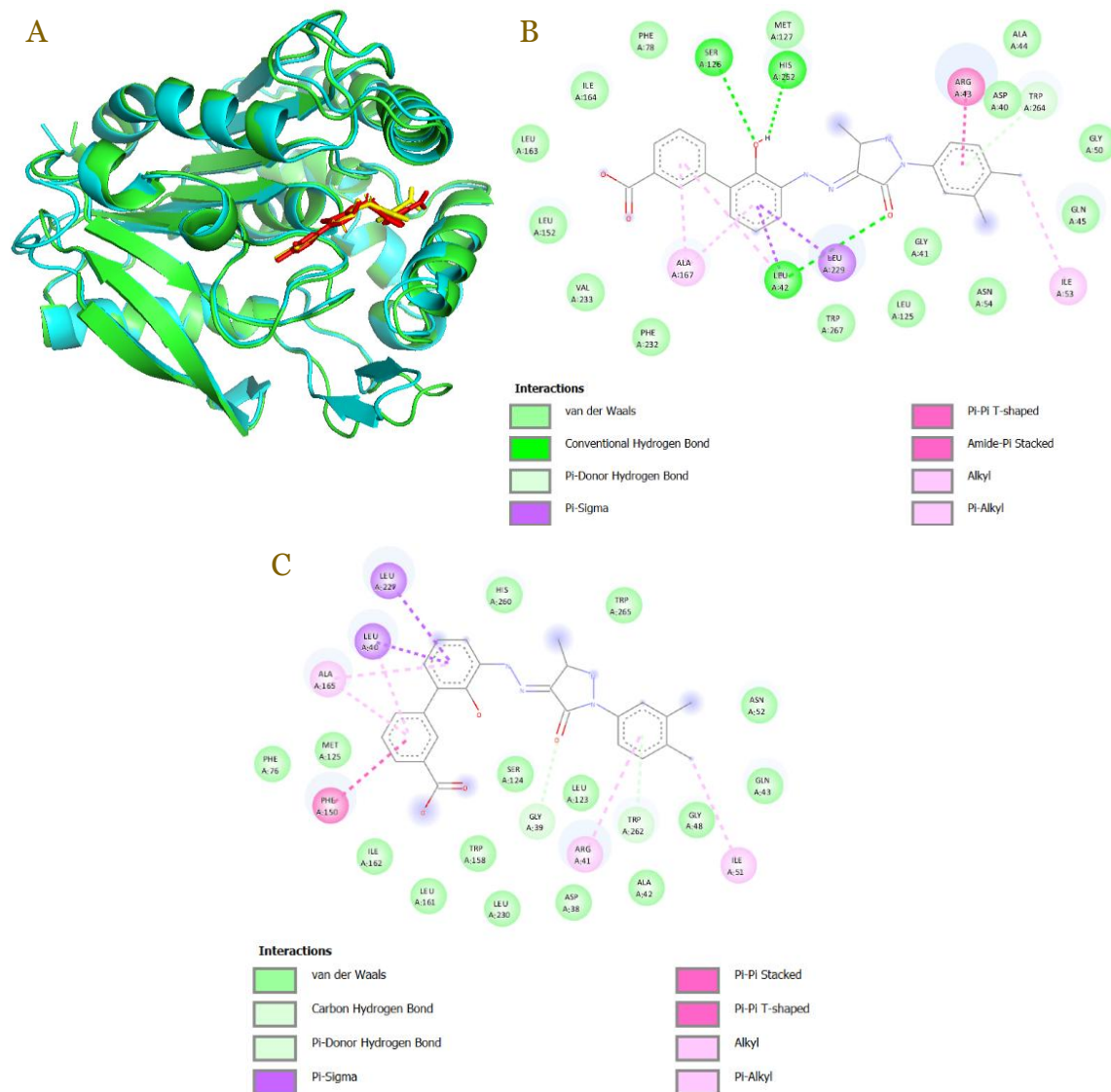


Figure 6. 3D visualization of eltrombopag and the Ag85B and Ag85C in superimposed form (A), 2D molecular interaction between imatinib with Ag85B (B), and Ag85C (C).

ADMET analysis

The ADME profiling involving the Lipinski rule of five properties and toxicity assessment showed that only a few compounds had passed the ADME screening, comprising approximately half of the listed drug-repurposed compounds. There are 30 compounds with molecular weights exceeding 500 Da, 10 with more than 10 Rotatable Bonds, and 16 and 13 exceeded the maximum number of hydrogen bond acceptors (HBA) and hydrogen bond donors (HBD), respectively. Thirty-five compounds were identified as having a high polar surface area (PSA) exceeding 140 \AA^2 , and eight were detected with high LogP values. Only some of the top potential compounds from docking studies, such as eltrombopag, pranlukast, and imatinib, have fulfilled the Lipinski rule of five assessments compared to other top compounds (**Underlying data**).

Table 3. Molecular Mechanics–Poisson–Boltzmann Surface Area (MM-PBSA) energies

Docked complex	Δ VDWAALS (kcal/mol)	Δ EEL (kcal/mol)	Δ EPB (kcal/mol)	Δ ENPOLAR (kcal/mol)	Δ EDISPER (kcal/mol)	Δ GGAS (kcal/mol)	Δ GSOLV (kcal/mol)	Total (kcal/mol)
Ag85A-selamectin	-41.72±3.15	-29.82±4.45	44.40±1.80	-5.22±0.13	0.00±0.00	-71.54±3.93	39.19±1.80	-32.35±3.30
Ag85A-imatinib	-49.34±3.23	-300.70±15.27	320.18±10.16	-5.65±0.09	0.00±0.00	-350.03±15.01	340.76±10.17	-9.27±8.14
Ag85B-imatinib	-50.70±2.27	-341.19±10.01	385.60±7.20	-5.59±0.04	0.00±0.00	-391.75±9.01	380.01±7.22	-11.74±4.97
Ag85B-eltrombopag	-46.74±0.98	-23.2±1.57	53.28±2.37	-4.95±0.08	0.00±0.00	-69.89±1.79	48.33±2.32	-21.55±2.55
Ag85B-trehalose (native ligand)	-39.53±1.15	-16.79±4.92	-32.44±3.43	-2.79±0.10	0.00±0.00	-37.37±5.15	-29.65±3.40	-7.72±3.00
Ag85C-eltrombopag	-50.74±2.66	-20.42±2.51	54.44±1.59	-4.79±0.05	0.00±0.00	-48.37±2.90	49.65±1.58	-21.52±2.86
Ag85C-imatinib	-48.31±3.05	-296.69±10.43	341.77±12.00	-5.31±0.08	0.00±0.00	-345.00±11.15	336.46±11.96	-8.54±3.86
Ag85B-CyC (native ligand)	-39.53±1.15	-16.59±2.67	38.62±3.74	-4.71±0.12	0.00±0.00	-56.12±3.23	33.91±4.24	-22.21±2.81

EDISPER: dispersion energy; EEL: electrostatic energy; ENPOLAR: non-polar solvation energy; EPB: polar solvation energy; GGAS: gas phase energy; GSOLV: solvation energy; VDWAALS: Van der Waals

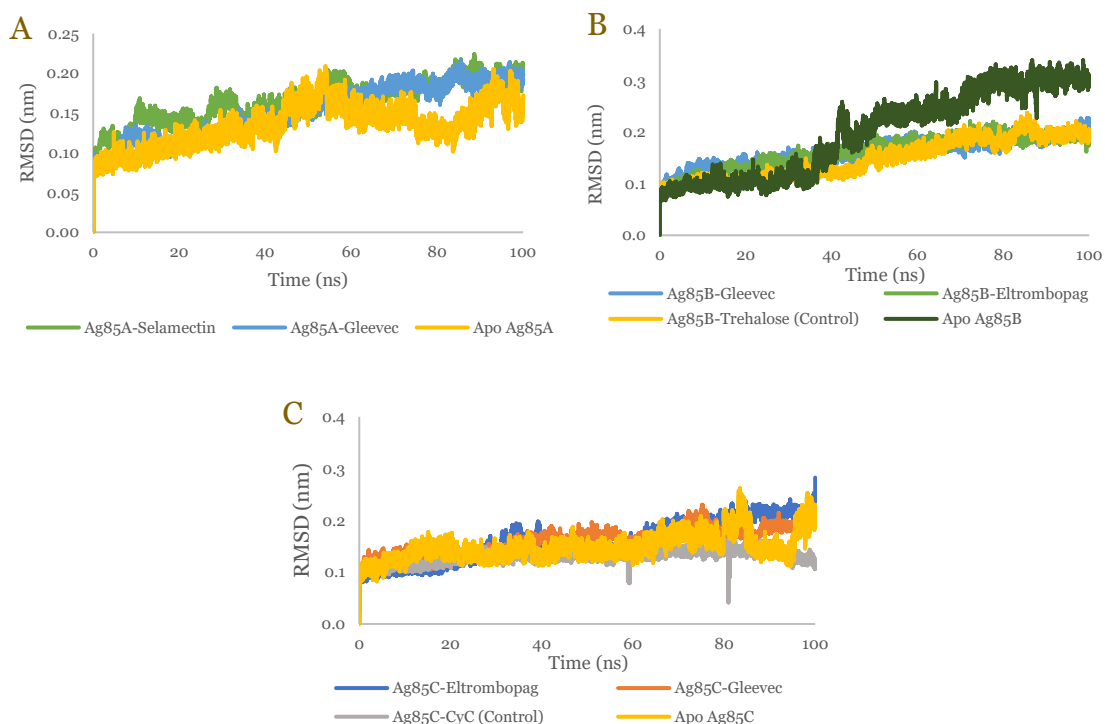


Figure 7. RMSD of three top candidates drug repurposed against Ag85 complex proteins during simulation. Ag85A complex with selamectin (light green), imatinib (blue) and apo form (yellow) (A), Ag85B complex with imatinib (blue), eltrombopag (light green), trehalose (yellow) and apo form (dark green) (B), and Ag85C complex with eltrombopag (blue), imatinib (orange), Cyc (grey) and apo form (yellow) (C).

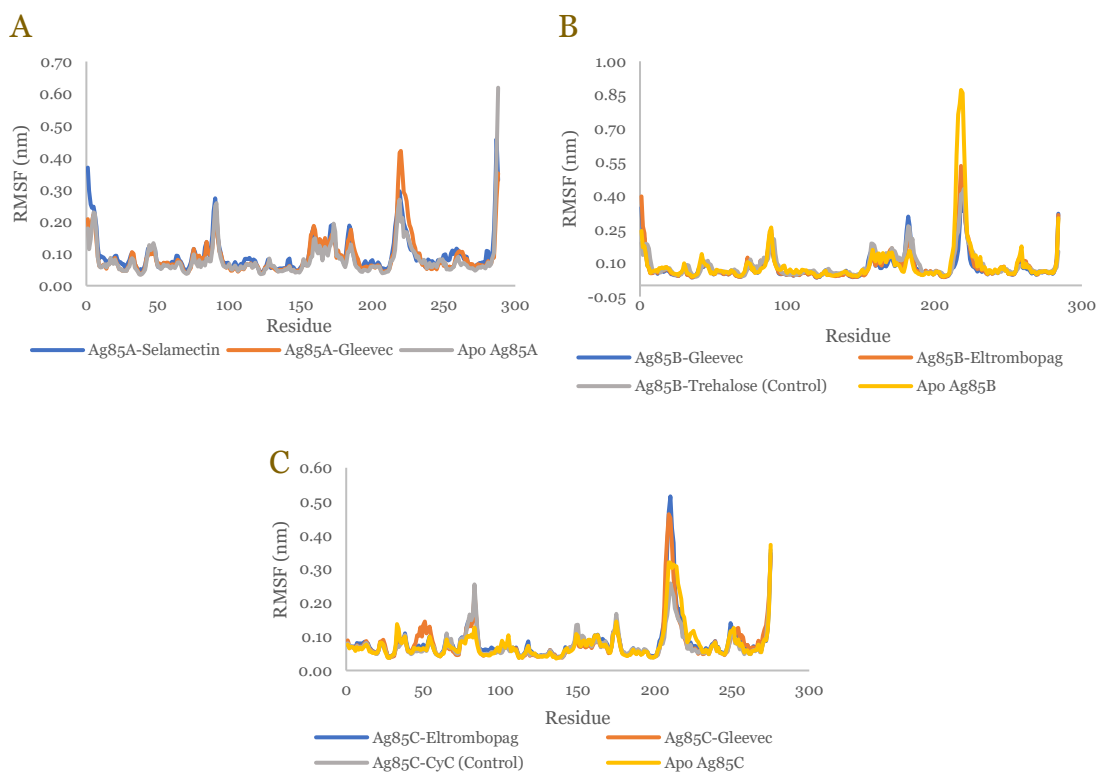


Figure 8. RMSF of three top candidates drug repurposed against Ag85 complex proteins during simulation. Ag85A complex with selamectin (blue), imatinib (orange) and apo form (grey) (A), Ag85B complex with imatinib (blue), eltrombopag (orange), trehalose (grey) and apo form (yellow) (B), and Ag85C complex with eltrombopag (blue), imatinib (orange), Cyc (grey) and apo form (yellow) (C).

Furthermore, in pharmacokinetic assays, among the top drug-repurposed lists, only Fluspirilene could pass the Blood-Brain Barrier. Additionally, some of the drugs could act as inhibitors for selected Cytochrome P450 (CYP450) enzymes that play essential roles in metabolism, which usually leads to a decrease in their activity and potentially affects how other drugs are metabolized, leading to possible drug-drug interactions (**Underlying data**) [25]. The rest of the compounds in the ADME analysis are listed in the **Underlying data**.

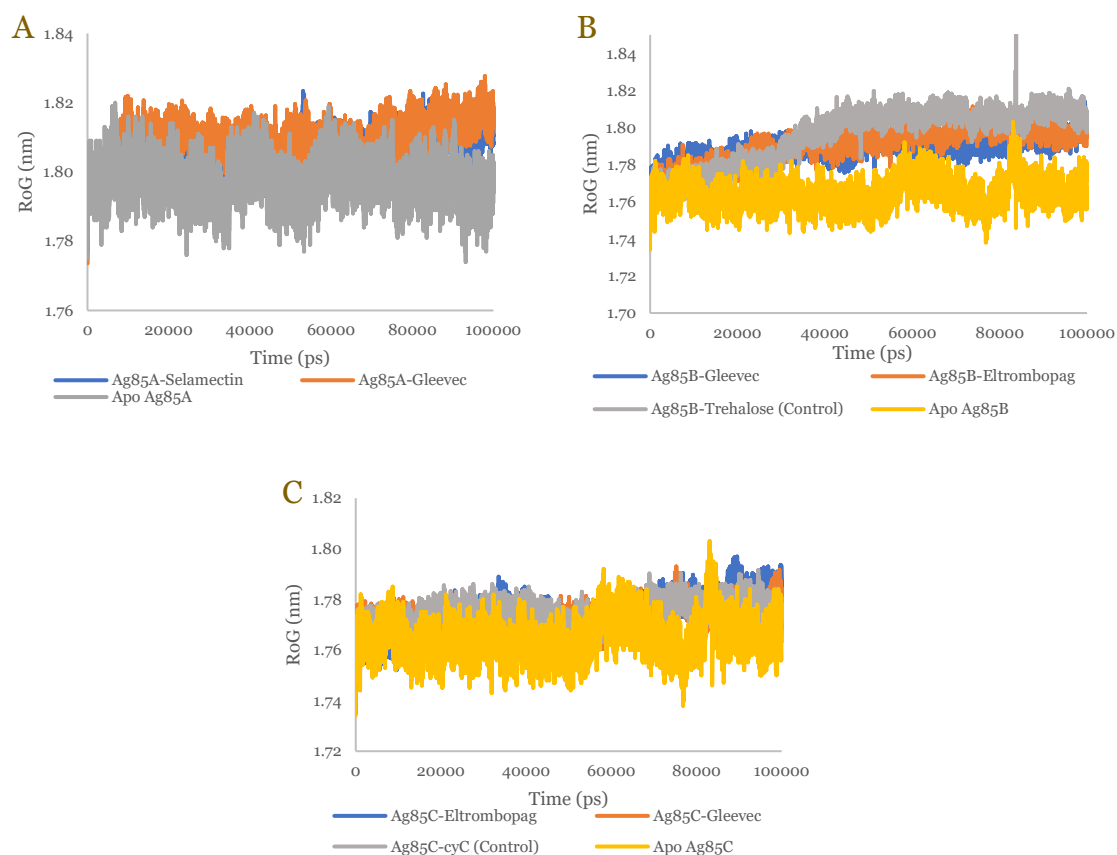


Figure 9. Radius of Gyration of three top candidates drug repurposed against Ag85 complex proteins during simulation. Ag85A complex with selamectin (blue), imatinib (orange) and apo form (grey) (A), Ag85B complex with imatinib (blue), eltrombopag (orange), trehalose (grey) and apo form (yellow) (B), and Ag85C complex with eltrombopag (blue), imatinib (orange), Cyc (grey) and apo form (yellow) (C).

Discussion

The molecular docking analysis in the present study revealed that nearly all of the repurposed drugs formed precise binding conformations at the active site, exhibiting higher binding affinity scores than the native ligands. Notably, the Ag85 complex proteins bound to the top 10 ligands displayed robust interactions with surrounding amino acids within a 5 Å radius of the active site, suggesting promising inhibitory effects on bacterial cell wall mechanisms. Even though ADME analysis identified that some of these drugs adhered to Lipinski's rule of five and exhibited favorable pharmacokinetic properties, among the top 10 candidate drugs, only eltrombopag was identified as a potential carcinogen based on the results of the pharmacokinetic analysis. Moreover, the top three drugs, selamectin, imatinib, and eltrombopag, exhibited the highest binding affinities from molecular docking with more than -10 kcal/mol scores compared to the co-crystallized ligands (trehalose and CyC). During simulations of three replicas, selamectin, imatinib, and eltrombopag showed stable behavior and favorable MM-PBSA free binding energy.

Besides its ability as an anti-parasitic drug, previous studies have shown that selamectin can act against *M. tuberculosis* and extensively inhibit clinical strains of Mycobacterium identified as resistant, including 27 MDR and XDR strains [26]. The activity of this drug type was also

reported, with the minimum inhibitory concentration ranging from 4–8 µg/mL against the *Mycobacterium* genus, and it was shown to be significantly effective when combined with rifampicin [27]. The most recent study on this drug revealed that in vitro analysis of selamectin and DprE1, an enzyme involved in mycobacterial arabinogalactan synthesis, suggests that this compound could be utilized as a multi-drug target in *Mycobacterium* species. The findings highlight selamectin's potential as a multi-target anti-mycobacterial compound, although its precise mode of action remains to be fully elucidated [28].

Likely, selamectin and imatinib (C₂₅H₂₂N₄O₄), have shown their ability against *M. tuberculosis* strains categorized as antibiotic-susceptible and resistant in MDR/XDR-TB since the target of imatinib is tyrosine kinases (TKs) and not bacterial factors. Therefore, the resistance mechanism from the bacteria is less than that of other antibiotics. This is followed by comparing the mutation rate between imatinib and first-line anti-TB drugs, which showed that imatinib can reduce the probability of mutations causing antibiotic resistance [29]. Furthermore, imatinib, also well-known as an anti-cancer and anti-tumor agent, is used to combat Abl and tyrosine kinases in leukemia and as host-directed therapy in mycobacterial infections [30]. The mechanism of this compound involves promoting acidification and maturation of phagosomes [31]. However, while imatinib shows promise as an adjunctive therapy for TB by enhancing immune response and managing granulomas, its immunosuppressive effects necessitate careful patient monitoring to mitigate the risk of TB reactivation in patients with latent infection [30].

Eltrombopag, a thrombopoietin agonist, has been shown to increase thrombocytopenia during TB treatment sufficiently. Its application in TB treatment is particularly relevant for patients suffering from immune thrombocytopenia with miliary tuberculosis [32]. A previous study also reported that eltrombopag may inhibit specific enzymes in *M. tuberculosis*, suggesting a dual role in both managing thrombocytopenia and potentially combatting TB infection directly [33]. However, the decision to use eltrombopag should be individualized according to the patient's condition due to the risk of thrombosis still exists for patients with chronic liver disease [34].

Based on these analyses, among 120 compounds, some of the compounds have shown promising results as the drug repurposed against Ag85 Complex. Although our hypothesis is determined by computational analysis, the number of compounds of TB drugs still needs to be explored and analyzed with more advanced molecular analysis. The study also still needs more analysis in developing the drug design prediction that combines the structure from the candidate compounds more comprehensively. Further analysis should, therefore, include in vitro and in vivo studies to ensure that the candidate drug-repurposed can inhibit Ag85 Complex, such as protein purification of Ag85 complex and ELISA studies.

Conclusion

This study has predicted 120 repurposed drugs that could potentially bind to the Ag85 complex proteins. Among the enlisted drugs, some were found to have more negative binding affinities and favorable interactions with each protein target, namely selamectin, imatinib, and eltrombopag. Molecular dynamics simulations further confirmed that these compounds could maintain stable and favorable interactions with Ag85 Complex proteins over time. However, this study still needs further analysis, particularly in vitro and in vivo studies, to determine the true potential of these compounds against Ag85 complex proteins in TB diseases.

Ethics approval

Not required.

Acknowledgments

The authors want to thank Pedro Ranault for his assistance in data analysis, the National for Research and Innovation Agency (Kemenristek/BRIN), and the StudiBio for the computational resources and support during the study.

Competing interests

All the authors declare that there are no conflicts of interest.

Funding

This work was supported by the Research and Innovation Agency (BRIN) through the grant of Research and Innovation for Advanced Indonesia (RIIM) with No.12/II.7/HK/2023 and the grant of Health Research Organizations in 2023 with No.23/III.9/HK/2023.

Underlying data

All underlying data can be assessed at <https://doi.org/10.5281/zenodo.11440772>. The file contains the list of compounds, molecular docking results, and ADMET analysis.

Declaration of artificial intelligence use

This study used artificial intelligence (AI) tools and methodologies in the following capacities: data analysis and modeling, data preprocessing, visualization and simulation and forecasting. We confirm that all AI-assisted processes were critically reviewed by the authors to ensure the integrity and reliability of the results. The final decisions and interpretations presented in this article were solely made by the authors.

How to cite

Iskandar IW, Nurhasanah A, Hatta M, *et al.* Computational drug repurposing for tuberculosis by inhibiting Ag85 complex proteins. *Narra J* 2025; 5 (1): e1130 - <http://doi.org/10.52225/narra.v5i1.1130>.

References

1. World Health Organization. Global tuberculosis report 2024. Geneva: World Health Organization; 2024.
2. Fahdhien F, Mudatsir M, Abidin TF, *et al.* Risk factors of pulmonary tuberculosis in Indonesia: A case-control study in a high disease prevalence region. *Narra J* 2024;4(2):e943.
3. Chai Q, Zhang Y, Liu CH. *Mycobacterium tuberculosis*: An adaptable pathogen associated with multiple human diseases. *Front Cell Infect Microbiol* 2018;8:158.
4. Cadena AM, Flynn JL, Fortune SM. The importance of first impressions: Early events in *Mycobacterium tuberculosis* infection influence outcome. *mBio* 2016;7(2):e00342-16.
5. Viljoen A, Richard M, Nguyen PC, *et al.* Cyclosporins and cyclophostin analogs inhibit the antigen 85C from *Mycobacterium tuberculosis* both in vitro and in vivo. *J Biol Chem* 2018;293(8):2755-2769.
6. Gagneux S. Ecology and evolution of *Mycobacterium tuberculosis*. *Nat Rev Microbiol* 2018;16(4):202-213.
7. Chowdhury K, Ahmad R, Sinha S, *et al.* Multidrug-resistant TB (MDR-TB) and extensively drug-resistant TB (XDR-TB) among children: Where we stand now. *Cureus* 2023;15(2):e35154.
8. Junaedi MA, Massi MN, Sjahril R, *et al.* Detection of katG, inhA and ahpC gene mutation in clinical isolates of isoniazid-resistant *Mycobacterium tuberculosis* in Makassar City, South Sulawesi, Indonesia. *Indian J Tuberc* 2024;71(4):383-388.
9. Muttaqin Z, Massi MN, Sjahril R, *et al.* Detection of rpoB gene mutations in clinical isolates of Rifampicin-resistant *Mycobacterium tuberculosis* in Makassar City, South Sulawesi, Indonesia. *Malays J Microbiol* 2023;19(4):380-384.
10. Ernst JD, Cornelius A, Bolz M. Dynamics of *Mycobacterium tuberculosis* Ag85B revealed by a sensitive enzyme-linked immunosorbent assay. *mBio* 2019;10(2):e00611-19.
11. Nisa A, Counoupas C, Pinto R, *et al.* Characterization of the protective immune responses conferred by recombinant BCG overexpressing components of *Mycobacterium tuberculosis* sec protein export system. *Vaccines* 2022;10(6):945.
12. Kruh-Garcia NA, Murray M, Prucha JG, *et al.* Antigen 85 variation across lineages of *Mycobacterium tuberculosis*—Implications for vaccine and biomarker success. *J Proteomics* 2014;97:141-150.
13. Fuchs M, Kämpfer S, Helmsing S, *et al.* Novel human recombinant antibodies against *Mycobacterium tuberculosis* antigen 85B. *BMC Biotechnol* 2014;14(1):68.
14. Gygli SM, Borrell S, Trauner A, *et al.* Antimicrobial resistance in *Mycobacterium tuberculosis*: Mechanistic and evolutionary perspectives. *FEMS Microbiol Rev* 2017;41(3):354-373.
15. Murphy B, Dempsey E. Evaluation of an Ag85B Immunosensor with potential for electrochemical *Mycobacterium tuberculosis* diagnostics. *ECS J Solid State Sci Technol* 2020;9(11):115011.
16. Xu Z, Hu T, Xia A, *et al.* Generation of monoclonal antibodies against Ag85A antigen of *Mycobacterium tuberculosis* and application in a competitive ELISA for serodiagnosis of bovine tuberculosis. *Front Vet Sci* 2017;4:107.

17. Kashangura R, Jullien S, Garner P, *et al.* MVA85A vaccine to enhance BCG for preventing tuberculosis. *Cochrane Database Syst Rev* 2019;2019(4):CD012915.
18. Kulkarni VS, Alagarsamy V, Solomon VR, *et al.* Drug repurposing: An effective tool in modern drug discovery. *Russ J Bioorganic Chem* 2023;49(2):157-166.
19. Pushpakom S, Iorio F, Eyers PA, *et al.* Drug repurposing: Progress, challenges and recommendations. *Nat Rev Drug Discov* 2019;18(1):41-58.
20. Kouznetsova VL, Zhang A, Tatineni M, *et al.* Potential COVID-19 papain-like protease PL^{pro} inhibitors: Repurposing FDA-approved drugs. *PeerJ* 2020;8:e9965.
21. Sharma K, Ahmed F, Sharma T, *et al.* Potential repurposed drug candidates for tuberculosis treatment: Progress and update of drugs identified in over a decade. *ACS Omega* 2023;8(20):17362-17380.
22. Aguilar Diaz JM, Abulfathi AA, Te Brake LH, *et al.* New and repurposed drugs for the treatment of active tuberculosis: An update for clinicians. *Respiration* 2023;102(2):83-100.
23. Sarkar A, Concilio S, Sessa L, *et al.* Advancements and novel approaches in modified AutoDock Vina algorithms for enhanced molecular docking. *Results Chem* 2024;7:101319.
24. Tang S, Chen R, Lin M, *et al.* Accelerating AutoDock Vina with GPUs. *Molecules* 2022;27(9):3041.
25. Zanger UM, Schwab M. Cytochrome P450 enzymes in drug metabolism: Regulation of gene expression, enzyme activities, and impact of genetic variation. *Pharmacol Ther* 2013;138(1):103-141.
26. Lim LE, Vilchère C, Ng C, *et al.* Anthelmintic avermectins kill *Mycobacterium tuberculosis*, including multidrug-resistant clinical strains. *Antimicrob Agents Chemother* 2013;57(2):1040-1046.
27. Omansen TF, Porter JL, Johnson PDR, *et al.* In-vitro activity of avermectins against *Mycobacterium ulcerans*. *PLoS Negl Trop Dis* 2015;9(3):e0003549.
28. Ezquerro-Aznárez JM, Degiacomi G, Gašparovič H, *et al.* The veterinary anti-parasitic selamectin is a novel inhibitor of the *Mycobacterium tuberculosis* DprE1 enzyme. *Int J Mol Sci* 2022;23(2):771.
29. Napier RJ, Rafi W, Cheruvu M, *et al.* Imatinib-sensitive tyrosine kinases regulate mycobacterial pathogenesis and represent therapeutic targets against tuberculosis. *Cell Host Microbe* 2011;10(5):475-485.
30. Cleverley TL, Peddineni S, Guarner J, *et al.* The host-directed therapeutic imatinib mesylate accelerates immune responses to *Mycobacterium marinum* infection and limits pathology associated with granulomas. *PLOS Pathog* 2023;19(5):e1011387.
31. Kim YR, Yang CS. Host-directed therapeutics as a novel approach for tuberculosis treatment. *J Microbiol Biotechnol* 2017;27(9):1549-1558.
32. Wada H, Sakashita T. A case of immune thrombocytopenia due to miliary tuberculosis effectively treated with eltrombopag. *Respir Med Case Rep* 2020;31:101320.
33. Battah B, Chemi G, Butini S, *et al.* A repurposing approach for uncovering the anti-tubercular activity of FDA-approved drugs with potential multi-targeting profiles. *Molecules* 2019;24(23):4373.
34. Mohamed SE, Yassin MA. Eltrombopag use for treatment of thrombocytopenia in a patient with chronic liver disease and portal vein thrombosis: Case report. *Case Rep Oncol* 2020;13(2):863-866.